Tropical Aquatic and Soil Pollution

Research Article
Volume 4(1), 2024, 27–42
https://doi.org/10.53623/tasp.v4i1.398

Stabilization of Pb, Cu, and Zn in Phytoaccumulator Ash in Calcined Clay-based Geopolymers and Potential Application

Samuel Sunday Ogunsola[1,2*], Adedeji Adebukola Adelodun[3], Mary Bosede Ogundiran[1]

[1]Analytical/Environmental Unit, Department of Chemistry, Faculty of Science, University of Ibadan, Ibadan, Nigeria
[2]Department of Chemistry and Biochemistry, Florida International University, Miami 33199, United States
[3]Department of Marine Science and Technology, Federal University of Technology, P.M.B. 704, Akure, Nigeria 340001

*Correspondence: samogery1250@gmail.com

SUBMITTED: 6 January 2024; REVISED: 4 April 2024; ACCEPTED: 7 April 2024

ABSTRACT: Following phytoremediation, the disposal of accumulating plants (phytoaccumulators) is challenging because the accumulated metals could leach back into the soil if not properly managed. Therefore, this study aims to use calcined clay (CC)-based geopolymer to stabilize Pb, Cu, and Zn in a phytoaccumulator (*Sporobolus pyramidalis*) ash (PA). Additionally, the effect of adding PA on the setting time, mechanical and heavy metals leaching properties of the geopolymers was investigated, to determine their environmental suitability and potential applications. Mixed proportions of CC (85-100%) and PA (5% - 15%) were used to produce geopolymers, using 8 M NaOH/Na_2SiO_3 (1:1) as an alkaline activator. The geopolymers were cured for 7 and 28 days at ambient temperatures. Thermograms showed the dehydroxylation of kaolinite at 450-650 °C. X-ray flourescene (XRF) analysis showed CC's predominant oxides as SiO_2 (53.1%) and Al_2O_3 (41.4%), while PA exhibited SiO_2 (46.6%), CaO (13.8%), PbO (1.30%), ZnO (0.28%), and CuO (0.04%). Thermal treatment eliminated most FTIR bands associated with kaolinite, converting crystalline kaolinite into amorphous metakaolinite. Geopolymer setting time ranged from 75 min (100% CC) to 111 min (85% CC). Furthermore, elevated Cao content in the PA resulted in the geopolymer's early strength development. However, the compressive strength decreased as PA quantity increased, with 95% CC-PA exhibiting maximum strength (22.5 ± 0.2 MPa) after 28 days. Further tests confirmed that 95% and 90% CC-PA geopolymer effectively stabilized Pb and Cu. Fabricated geopolymers met the ASTM (C62-17) Specification Standard for building brick, indicating their suitability as a waste-based construction material under controlled conditions.

KEYWORDS: Phytoremediation; *Sporobolus pyramidalis*; phytoaccumulator ash; calcined clay-based geopolymer; waste-based construction material

1. Introduction

Due to ever-growing industrialization and inappropriate waste management, heavy metal pollution has become an incessant global problem. Unlike organic pollutants, heavy metals are

non-biodegradable; hence, they are environmentally refractory [1, 2]. Eventually, these metals biomagnify along the food chain, making man the terminal target. Even at trace concentrations, they are hazardous to human health [3, 4]. For instance, the regulatory limit for lead (Pb) and copper (Cu) in drinking water, as defined by the US Environmental Protection Agency (EPA), is 0.05 mg/L and 1.3 mg/L, respectively [5, 6]. Additionally, the World Health Organization (WHO) recommends safe limits for Pb in wastewater and soils used for agriculture at 0.01 mg/L and 0.1 mg/L, respectively [7]. Therefore, various scientific efforts have effectively removed them from the environment. Such efforts include the use of physical [8, 9], chemical [3, 10], and biological [11, 12] remediation methods.

One of the economically viable, cost-effective, and environmentally benign technologies to mitigate heavy metal pollution in soils is phytoremediation [13–18]. Phytoremediation is a green technology whereby plants (i.e., phytoaccumulators) partially or completely remediate contaminated sites [13, 14, 17, 19]. Usually, various plant's physical and biological properties are exploited for this purpose [20]. If the accumulators are properly managed, polluted soils can be effectively restored to their "status quo". After the advent of phytoremediation, researchers have raised concern regarding the death of accumulator plants on-site or during their transfer to alternate environments for disposal. These could lead to the release of accumulated metals back into the soil [21, 22], causing significant soil and groundwater pollution [3, 23]. Therefore, the pressing need for techniques to stabilize or immobilize phytoaccumulated metals has become exigent. One such technique is the use of geopolymers.

Primarily, geopolymers were developed as a substitution for Ordinary Portland Cement (OPC), with the main goal of diminishing the excessive release of CO_2 associated with the production of OPC. This approach also sought to curtail the consumption of natural resources and energy expended in its production [24], Additionally, geopolymers have demonstrated a stabilization/immobilization mechanism akin to the OPC binding processes for encapsulation [25]. However, they show superior chemical and physical properties in compressive strength, durability over a long time, resistance to fire and acid attacks, structural integrity, and shrinkage resistance. All these properties depend on the starting material and the processing condition [26].

Over the past few decades, researchers have immensely explored the utilization of geopolymers for heavy metal stabilization/immobilization purposes in waste materials [25, 27–32]. Geopolymers are amorphous equivalents of zeolitic materials usually produced from a reaction that involves alkali activation of aluminosilicate materials, such as metakaolin clay, blast furnace slag, and fly ash. The reaction yields an aluminosilicate gel that is alkaline in nature, exhibiting a three-dimensional solid structure wherein both Si and Al are coordinated in tetrahedral arrangements [33–35]. During heavy metal stabilization [18, 36], aluminosilicate materials, which might include waste materials, are alkali activated. In this process, binders are produced and subsequently mixed with hazardous wastes to reduce the leaching of contaminants, transforming the hazardous waste into a more environmentally suitable form for disposal on land or use in construction. For instance, Ogundiran et al. [36] used waste aluminum anodizing etching solution (AES) as an activator to produce fly-ash geopolymers in place of the common silicate solution. Their result revealed that heavy metals were well immobilized in the fabricated binder. El-Eswed et al. [37] utilized kaolin/zeolite-based geopolymers to stabilize Pb^{2+}, Cd^{2+}, Cu^{2+}, and Cr^{3+}. Earlier, Phair et al. [38] also stabilized Pb and Cu in fly-ash-based geopolymer.

Majorly, geopolymers have garnered attention for Pb immobilization because Pb negatively impacts the hydration and setting of other binders like OPC [39]. This phenomenon is attributed to developing impermeable layers around the clinker grains [40]. Several observations have been published to explain the mode of heavy metal (specifically Pb) immobilization in geopolymers. Pandey et al. [41] suggested that the elevated synthesis pH caused the formation of insoluble metal-hydroxides, which were then enclosed within the amorphous aluminosilicate framework of the geopolymers. Many authors have reported the same opinion [25, 28, 29]. Pb may also precipitate as lead-silicate [40] or participate in charge equilibrium by substituting for Na^+ within the structure [25, 42]. According to Cheng et al. [43], during diffusion into geopolymer, the Pb^{2+} could stay entrapped in the pores, reducing its leachability. Van Jaarsveld et al. [44] reported that the immobilization of Cu and Pb in fly ash-based geopolymer could be due to chemical bonding, physical encapsulation, and chemical adsorption.

Furthermore, it has been reported that geopolymers exhibit considerable immobilization capacity for Zn (II) [45–47, 49]. Li et al. [1] synthesized geopolymer from electrolytic manganese residue and lead-zinc smelting slag. The synthesized geopolymers were successfully used to immobilize Pb^{2+} and Zn^{2+}. The authors reported that the geopolymers with 1% Pb exhibited the highest compressive strength of 28.5 MPa after seven days of curing. Most authors believed that physical encapsulation is the leading cause of heavy metal immobilization in geopolymers [25, 28, 29, 38, 50, 51]. However, a contrary opinion was reported [48]. The team hypothesized that Pb and Cu serve to offset the negative charge associated with tetrahedral Al within the geopolymer frameworks, with no emphasis on physical encapsulation. Therefore, the precise mechanism for immobilizing heavy metals in geopolymers remains incomplete [24, 45, 50]. Nevertheless, several factors could affect the immobilization of heavy metals in geopolymers [24]. These factors encompass the features of heavy metals and their forms, the attributes of the source materials, and the pH and type of alkali activator used.

Aside from heavy metal immobilization, geopolymers have also reportedly been used to immobilize/stabilize toxic and radioactive wastes [51, 53–55]. To our knowledge, there have been no reports regarding the utilization of geopolymers for the stabilization or immobilization of phytoaccumulated heavy metals. Therefore, this research aimed to present the first attempt at using CC-based geopolymer to stabilize and immobilize three heavy metals (Pb, Cu, and Zn) accumulated in a plant (giant rat's tail grass) that grew naturally on heavy metal-polluted soil. Further, the structural (mechanical) effect of the PA as a component of fabricated geopolymer was studied.

2. Materials and Methods

2.1. Sampling and sample pretreatment.

A Nigerian kaolin clay, called Ikere-kaolin clay, was obtained from a natural deposit in Ikere-Ekiti, Ekiti State of Nigeria. The location lies at longitude 7º 2'N and latitude 5º 91'E. The raw kaolin clay sample was pretreated as reported by Ogundiran and Ikpeni [18]. Briefly, the raw natural clay was sun-dried and crushed with a rolling rod, followed by air-drying for one week and sieving to 212 µm using an Endicott Ltd, London, stainless steel sieve. The sieved clay was thermally treated in an electric furnace at 650°C for 6 hrs to convert it to the more reactive metakaolin used for geopolymer production.

A heavy metal-accumulating plant, giant rat's tail grass (*Sporobolus pyramidalis*) [56], was obtained at different distances and along three (3) directions: west, north, and north-east from a lead-smelting slag polluted site in Lalupon, Ibadan, Nigeria. *Sporobolus pyramidalis* can accumulate significant heavy metal levels, making it a potential phytoremediator [56]. The accumulator was gently but thoroughly washed with distilled water at the lab before air-drying for two weeks. Then, it was ashed in a muffle furnace at 650° C for 6 hrs before cooling to room temperature. The PA ash was stored in a desiccator for analysis and future use.

2.2. Physical and chemical characterization.

The thermal reactions of the kaolin clay to determine its dehydroxylation temperature were done using thermogravimetric analysis coupled with differential thermal analysis (TGA/DTA) (NETZCHDTA, 404 PC, Germany). This study focuses exclusively on acquiring the dehydroxylation temperature data for the kaolin clay. A constant temperature of 650° C was sustained for 6 hrs. to guarantee the thorough ashing of the phytoaccumulator [56]. Chemical characterization was done using an Energy Dispersive X-ray Fluorescence Spectrometer (EDX3600B) and Fourier Transform-Infrared (FT-IR) Spectroscopy (Perkin Elmer Inc – spectrum BX FTIR spectrometer, USA).

2.3. Production and characterization of the geopolymer.

A solution mixture 1:1 (w/w) of sodium silicate (Na_2SiO_3; chemical composition of 30.1% SiO_2, 9.4% Na_2O, and 60.5% H_2O) and 8 M NaOH (Sigma Aldrich, 97.9%) was used as an alkaline activator. The alkaline activator was left for 24 hrs. at room temperature before use. The percentage proportion of CC to PA was 100%, 95%, 90%, and 85%. The initial mass of the 100% clay sample was 90 g. Consequently, all subsequent calculations were based on this reference point. The mix proportion and predetermined quantity of activator used for each percentage ratio are presented in Table 1. The higher the CC, the higher the activator that was enough to prepare the geopolymer. This observation is because clay, characterized by its plate-like particle shape, requires high water demand during geopolymer formation [57–59]. The CC and PA were dry mixed in a mixer for 3 min to homogenize. The alkali activator was added to the homogenized sample and mixed again for 20 min until a thixotropic paste was obtained. The pastes were cast into a cube mold (40 mm × 40 mm × 40 mm) and vibrated on a table for 5 min to enhance compaction and remove entrapped air [60]. The setting time of the pastes was determined as the time elapsed between molding and the onset of hardening, i.e., when needle penetration was no longer possible [25]. The Vicat needle experiment ASTM C187/C191 [61] was conducted every 15 minutes after curing. Subsequently, the geopolymer paste was cured in a sealed plastic bag at ambient temperature to prevent the evaporation of mixing water and the carbonation of the surface [34, 62, 63]. After three (3) days, it was de-molded after three days for subsequent testing. In addition, an unstabilized (unactivated) counterpart of each CC-PA geopolymer was prepared.

The compressive strength of the geopolymers was assessed after curing for 7 and 28 days. Three separate geopolymer samples were tested using a compression test machine (ELE International, ADR Touch, 2000, UK). In each test, the maximum force needed to reach the fracture point was divided by the cross-sectional area of the geopolymers. The average of the two most proximate outcomes was computed and recorded as the compressive strength of the geopolymers [18].

Table 1. Mix proportion used on a weight basis to produce geopolymers to prepare CC-PA geopolymers.

S/N	Sample ID (%)	CC (g)	PA (g)	Activator (g)	Activator/solid ratio
1	100%	90.0	0.00	74.0	0.82
2	95%	85.5	4.50	65.0	0.72
3	90%	81.0	9.00	63.0	0.70
4	85%	76.5	13.5	62.0	0.68

2.4. Toxicity characteristics leaching procedure test (TCLP).

The efficiency of heavy metal stabilization or immobilization is determined by the metal's strength and resistance to leaching [64]. Therefore, the leaching test is probably the most effective method to determine the heavy metal stabilization degree. Several leaching techniques have been utilized to gather information for environmental decision making [25]. However, The TCLP best determines the mobility of contaminants in solid, liquid, and multi-phased wastes. It also simulates the worst-case scenario for waste disposal in landfills [65]. In a prior investigation conducted by [18], they replaced kaolin clay with waste materials in the range of 0-20%, and the TCLP was effectively employed to quantify the leachable heavy metals. Therefore, the TCLP method (USEPA Method 1311) was conducted in this work to ascertain the binding capacity of the CCPA-based geopolymer as an immobilizing material for Pb, Cu, and Zn [25, 36, 38] and to assess the environmental fitness of CC-PA geopolymers for potential uses.

To ensure the sample's representativeness, the geopolymer samples were first crushed and thoroughly homogenized using the quaternary method. Subsequently, 2.0 g of material with particle sizes less than 9.5 mm was carefully selected from the homogenized sample and used for triplicate analysis. The extraction process was done using 40 mL of 0.1 M acetic acid solution (pH = 2.88 ± 0.05) in capped polyethylene centrifuge tubes. The acidic pH was preferred for the extraction because of the samples' highly alkaline nature (pH = 12.00 ± 0.05), which could precipitate the metal ions as hydroxides. However, the acidity of the unstabilized samples was about pH = 6.20 ± 0.02. Therefore, it was extracted with sodium/acetic acid solution (pH = 4.93 ± 0.05). In both instances, the extraction vessels were subjected to end-to-end shaking at 30 rpm for 18 hrs. Subsequently, the mixture was filtered to eliminate any suspended solids. The resulting filtrates were acidified with HNO_3 until the pH reached below 2 before instrumental analysis to prevent the formation of precipitates. Finally, Flame Atomic Absorption Spectrometer (FAAS) (A-analyst 200, UK) quantified the leachable heavy metals in the samples.

3. Results and Discussion

3.1. Characterization of materials.

The TGA/DTA result (Fig. 1) shows an endothermic peak within 450 – 650 ºC, indicating the simultaneous dehydroxylation of the kaolinite in the clay to form metakaolinite [34]. This endothermic peak also indicates the calcination temperature. Therefore, the clay was thermally treated in a muffle furnace at 650 ºC for 6 hrs. The IR spectra of raw clay and CC are presented in Fig. 2. The raw clay exhibits a sharp peak at 3686 cm^{-1}, corresponding to the stretching vibrations of OH bonds attached to the Al octahedron sheet. The peak at 1633 cm^{-1} can be attributed to the bending vibration mode of physisorbed water on the surface of free silica produced due to Al removal [66]. The band associated with Si-O-Si stretching or Si-O-Al was

seen at 1046 cm^{-1}, whereas those associated with Si-O stretching and Al (vi)-O-Si bending vibrations were observed at 786, 758, and 685 cm^{-1}. According to Ogundiran and Kumar [59], the band at 472 cm^{-1} is attributed to Si-O stretching vibrations in kaolinite. However, upon calcination, most of these kaolinite bands, such as the OH bands at 3686 cm^{-1} and the physisorbed water vibration mode band at 1633 cm^{-1}, vanished [66]. Moreover, significant transformations occurred at lower wavenumbers below 1400 cm^{-1}, including the disappearance of the Al-O-Si bands at 758 and 783 cm^{-1}, indicating the conversion of kaolinite to the more reactive metakaolinite. The XRD analysis from previous studies has confirmed that the metakaolinite product of the Ikere kaolin clay is amorphous [59], [34]. The band observed at 3453 cm^{-1} has been ascribed to atmospheric water The band observed at 3453 cm^{-1} has been ascribed to atmospheric water [67].

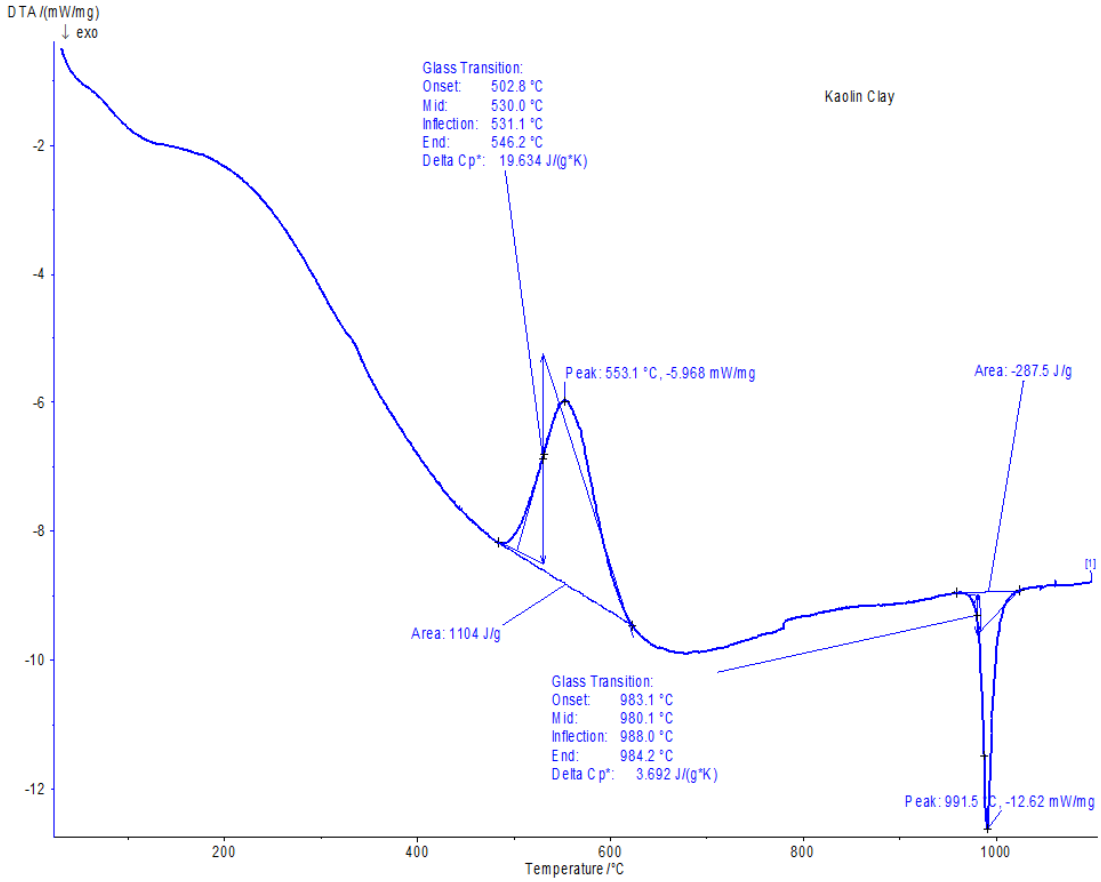

Figure 1. Differential thermal analysis (DTA) curve of raw Ikere-kaolin clay.

Furthermore, the oxide composition (XRF) results of the CC and PA are shown in Table 2. The CC consists mainly of SiO_2 (53.1%) and Al_2O_3 (41.4%). These oxides are the building blocks of geopolymer formation [34], making the clay a potential candidate as a geopolymer precursor. Moreover, the composition of the oxides indicated that the raw clay is not a purely kaolinite-containing type but rather consists of trace amounts of other minerals. The PA consists mainly of SiO_2 (46.6%) and CaO (13.8%). The high CaO content indicates a significant calcite amount [68]. PbO (1.30%), ZnO (0.28%), and CuO (0.04%) are also present in considerable quantity.

Table 2. Chemical composition (% wt.) of the CC and PA.

Oxide	CC	PA
Al_2O_3	41.4	6.77
SiO_2	53.1	46.6
P_2O_5	0.19	1.61
SO_3	0.74	8.12
K_2O	0.11	10.5
CaO	0.06	13.8
TiO_2	0.23	-
Fe_2O_3	0.61	5.72
NiO	0.06	0.05
CuO	-	0.04
ZnO	0.11	0.28
PbO	0.02	1.30
WO_3	0.04	0.26
MoO_3	0.23	0.36
SnO_2	1.53	1.84
Sb_2O_3	1.43	1.66

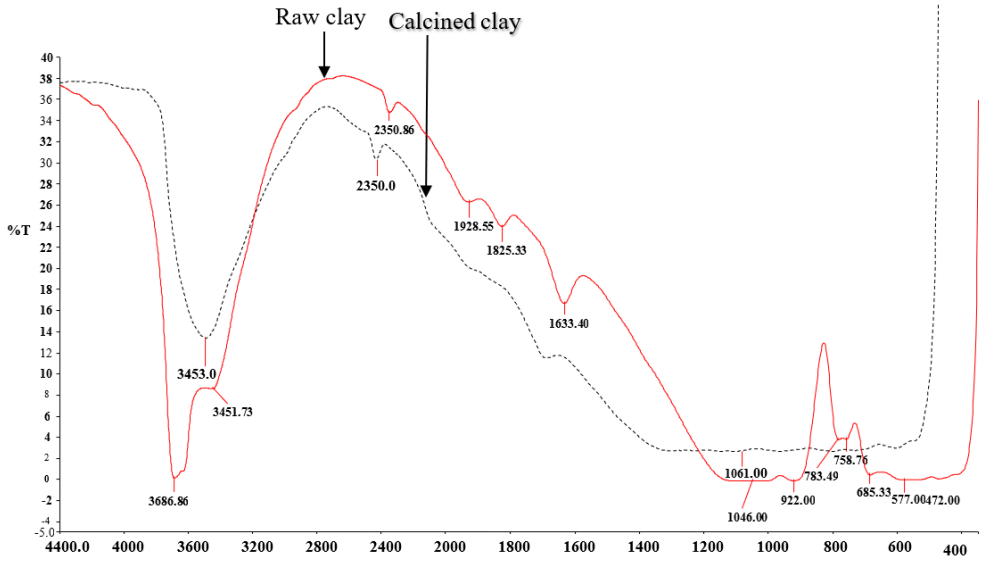

Figure 2. The FTIR spectra of Ikere-Ekiti raw clay (red line) and CC (black line).

3.2. Characterization of the geopolymers.

3.2.1. Setting time.

The setting duration of metakaolin-based geopolymer is influenced by the choice of raw materials and the proportions used in the mixture [69]. In this work, the setting time of the geopolymers (Fig. 3) increased with PA quantity. This trend could be attributed to the fact that silicate species in the alkaline activator solution was the most reactive. However, in this study, as the amount of PA increases, the quantity of activator needed to produce the geopolymer decreases. As a result, the solution's reactivity diminishes due to the reduced activator content, leading to a slower dissolution of silicates and aluminates in both the CC and PA. Consequently, an extended setting time was observed with an increase in PA. Additionally, geopolymers' setting time could increase with increased SiO_2/Al_2O_3 ratios [70] because a significant quantity of soluble silica within the alkaline solution boosts geopolymerization. Therefore, the reaction requires additional time to solidify and strengthen, resulting in an extended geopolymer setting period [71]. Thus, the elevated SiO_2/Al_2O_3 ratio of the PA (6.8) (Table 2) could be responsible for the trend observed here, indicating a slow activation of the

geopolymer paste with increased PA content. It is worth mentioning that some research works linked this type of trend to the SiO_2/Al_2O_3 ratio. For example, Silva et al. [70] explored the influence of the SiO_2/Al_2O_3 ratio on the setting duration of metakaolin-based geopolymers. They observed that raising this ratio from 2.5 to 5.01 extended the geopolymer's setting time. In another work, Siyal et al. [71] discovered that augmenting the Si/Al ratio from 1.8 to 2.2 increased the geopolymer's setting time. Such an occurrence could be advantageous because a retarded setting time allows for the complete dissolution of the material [25]. Hence, improved workability of the geopolymer paste for an extended period was achieved [72].

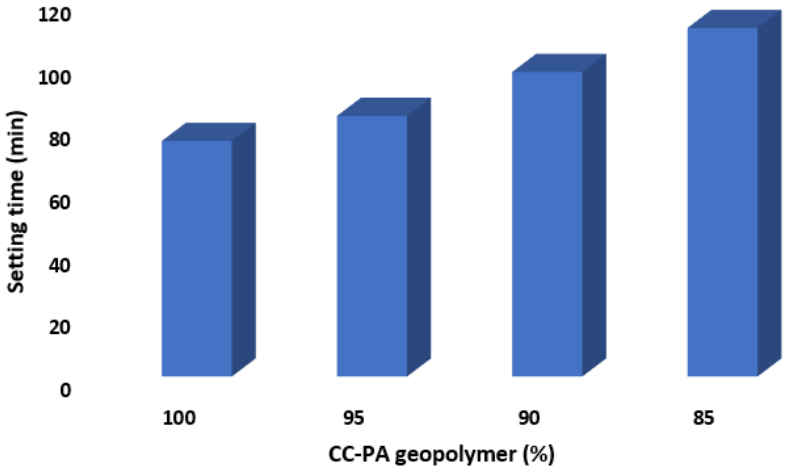

Figure 3. Setting time of CC-PA geopolymers.

3.2.2. Compressive strength.

The compressive strength of the geopolymers of various proportions of CC and PA at 7 and 28 days is shown in Table 3**.** It was observed that the compressive strength of the geopolymer progressively increased with the curing duration. Moreover, a notable advancement in early strength was observed during the initial 7-day period for geopolymers incorporating PA. This result underscores the role of the high CaO content in the PA, facilitating the binder material reaction thereby spearheading early strength development [73]. It has been reported that calcium content significantly influences the properties of fresh mixture and final hardened products [74], [75]. Table 3 shows that geopolymers with PA gained more than 80% of their strength within seven days of curing. In their experiments, Wijaya et al. [76] reported a similar observation when they discovered that paste with a CaO content exceeding 20% achieves 54% of its 28-day strength in just three (3) days. Also, Seo et al. [77] reported an early compressive strength when they incorporated CaO into a ternary blend Portland cement-slag-silica fume system, at room temperature.

Table 3. Compressive strength (MPa) of CC- PA-based geopolymers at 7 and 28 days of curing.

Curing days	100%	95%	90%	85%
7	20.8 ± 0.3	18.0 ± 1.5	15.9 ± 5.2	9.46 ± 2.9
28	38.0 ± 2.4	22.5 ± 0.2	19.0 ± 0.5	9.86 ± 0.9

In this study, the 100% CC geopolymer showed the highest strength of 38.0 ± 0.2 MPa, similar to 35 N/mm^2 reported by Elimbi et al. [78] for kaolin clays calcined at 650^o C. Furthermore, among the fabricated geopolymers, the 95% geopolymer demonstrated the highest compressive strength of 22.5 ± 0.2 MPa after 28 days of curing, meeting the ASTM

(C62-17) [79] Specification Standard (20.7 MPa) for building bricks under severe weathering conditions. Conversely, the 90% geopolymer exhibited a compressive strength of 19.0 ± 0.5 MPa, surpassing the required 17.2 MPa for moderate weathering [80]. This outcome suggests their suitability as a waste-based construction material under controlled conditions. However, compressive strength decreased with the increase in PA proportion. This trend can be attributed to the decreased amount of activator needed to produce geopolymers when there is an increase in PA. A similar observation was recently published [81]. The authors reported reduced geopolymer compressive strength with increased periwinkle shell ash. They linked this observation to the elevated calcium ions present in the periwinkle shell. Therefore, it is essential to note that while CaO content influences early strength development, an elevation in the CaO content could potentially decrease the strength of the geopolymers [82], [81]. Also, the substantial quantity of SiO_2 in PA (Table 2) could be responsible for this observation. An elevated Si/Al ratio could diminish the ability of the geopolymeric gels, leading to the presence of some unreacted Si, which may be soft and act as a defect in the geopolymer binder [83], [84].

3.2.3. Toxicity Characteristic Leaching Procedure (TCLP).

The TCLP results of the fabricated geopolymer and its unstabilized counterparts are presented in Table 4. The unstabilized counterpart is a mixture of the PA and CC (Table 1) without the activator. This test was conducted to investigate the effectiveness of the geopolymer network in binding the heavy metals in PA as an alternative way of managing phytoaccumulators and to assess the ash-containing geopolymers' environmental suitability. Cu and Pb were not detected in the CC sample without PA. The leachable Pb ranged from 0.09-0.32 and 0.28-1.75 mg/l in the geopolymer and unstabilized counterparts, respectively. While Cu was not detected in the geopolymer leachates, indicating that its concentration remained below the 1.3 mg/l permissible limit recommended by USEPA for drinking water [5], [6], the Pb levels in all the leachates still exceeded the safe limit for Pb in wastewater set by WHO, which is 0.01 mg/l. However, the 95% CC' leachate exhibited a Pb concentration of 0.09 ± 0.01, statistically equal to the limit (0.1 mg/l) set by WHO for agricultural soils [7]. The leachable Zn concentration ranged from 0.22 (100%) to 0.42 and 0.32-0.43 mg/l in the geopolymer and unstabilized counterparts, respectively. This result suggests that Zn was not effectively stabilized within the geopolymer network.

Table 4. Leachable heavy metal concentrations (mg/L) in TCLP leachates of CC-PA geopolymers and their unstabilized counterparts.

S/N	Sample subjected to TCLP test Geopolymers	Pb	Cu	Zn	%Pb	%Cu	%Zn
		Mean conc. in samples (mg/l)			% reduction in conc. due to stabilization		
1	100%	ND	ND	0.22 ± 0.01			
2	95%	0.09 ± 0.01	ND	0.32 ± 0.03	68.0	100	21.9
	Unstabilized counterpart	0.28 ± 0.02	0.03 ± 0.01	0.41 ± 0.02			
3	90%	0.19 ± 0.01	ND	0.34 ± 0.04	94.5	100	20.9
	Unstabilized counterpart	1.65 ± 0.15	0.03 ± 0.00	0.43 ± 0.02			
4	85%	0.32 ± 0.00	ND	0.42 ± 0.03	81.7	100	2.33
	Unstabilized counterpart	1.75 ± 0.08	0.03 ± 0.00	0.43 ± 0.04			

ND = Not Detected; Detection limits (mg/l) of the instrument for Cu = 0.0025, Pb = 0.018, Zn = 0.006.

Nevertheless, it was observed that immobilizing the leachable Pb, Cu, and Zn through stabilization lowered the concentration of the heavy metals in the geopolymers than in the unstabilized counterparts. All the CC-PA-based geopolymers showed higher binding capacities for Cu and Pb than Zn. With the unstabilized counterparts, the CC-PA-based geopolymer exhibited 100% and 86% binding capacities for Cu and Pb, respectively. Overall, up to 94.5% and 100% of Pb and Cu were respectively immobilized in the 90% geopolymer. These findings demonstrate the potential of CC geopolymer to successfully stabilize Cu and Pb within PA, effectively mitigating the leaching of these metals.

4. Conclusion

The Stabilization/immobilization of Pb, Cu, and Zn in PA using a CC-based geopolymer was studied. There was a direct correlation between the quantity of PA and the setting time of geopolymers, which can be linked to the notable Si/Al ratio within the PA. Moreover, the increased presence of CaO in the PA expedited the initial strength development of the geopolymer. There was a significant decrease in the concentration of Pb and Cu in 95% and 90% geopolymers. Hence, the geopolymer network was effective in binding Pb and Cu. However, Zn was not adequately immobilized within the geopolymer network. The compressive strength of the CC-PA geopolymer decreased with increased PA proportion. However, 90% and 95% of the geopolymers satisfied the ASTM specification standard for building bricks under moderate and severe weathering conditions, respectively. Consequently, CC-based geopolymer can effectively immobilize Pb and Cu in PA while maintaining good mechanical properties. Additional research is necessary to determine the impact of PA on other geopolymer properties, including water absorption and dry density. Also, the prolonged setting time could be attributed to the increase in the SiO_2/AlO_3 ratio. However, it could not be ascertained in this current study. Along with other textural and physiological characterization, detailed XRD analysis of the PA in our future work would comprehensively confirm any attribution made in this respect." Furthermore, a more profound comprehension of the geopolymerization reactions involving PA is imperative.

Author contributions: Samuel S. Ogunsola: Conceptualization, Data curation, Writing-original draft, resources, Investigation; Adedeji A. Adelodun: Writing-Review and editing; Mary B. Ogundiran: Conceptualization, Validation, Writing-Review and editing, Supervision, Resources, Methodology.

Competing Interest

No potential conflict of interest was reported by the authors.

References

[1] Li, M.; Kuang, S.; Kang, Y.; Ma, H.; Dong, J., et al. (2022). Recent advances in application of iron- manganese oxide nanomaterials for removal of heavy metals in the aquatic environment. *Science of The Total Environment, 819*, 153157. https://doi.org/10.1016/j.scitotenv.2022.153157.

[2] Zhang, Y.; Wang, Y.; Zang, H.; Yao, J.; Ma, H. (2023). Analysis of Heavy Metal Pollution in Soil along the Shuimo River by the Grey Relational Method and Factor Analysis. *Metals*, *13*(5), 878. https://doi.org/10.3390/met13050878.

[3] Ogunsola, S.S.; Oladipo, M.E.; Oladoye, P.O.; Kadhom, M. (2024). Carbon nanotubes for sustainable environmental remediation: A critical and comprehensive review. *Nano-Structures & Nano-Objects*, *37*, 101099. https://doi.org/10.1016/j.nanoso.2024.10109.

[4] Mishra, S.; Bharagava, R.N.; More, N.; Yadav, A.; Zainith, S., et al. (2019). Heavy Metal Contamination: An Alarming Threat to Environment and Human Health. In *Environmental Biotechnology: For Sustainable Future* (pp. 103–125). Springer Singapore.

[5] Taylor, A.A.; Tsuji, J.S.; Garry, M.R.; McArdle, M.E.; Goodfellow, W.L., et al. (2020). Critical Review of Exposure and Effects: Implications for Setting Regulatory Health Criteria for Ingested Copper. *Environmental Management*, *65*(1), 131–159. https://doi.org/10.1007/s00267-019-01234-y.

[6] Goel, J.; Kadirvelu, K.; Rajagopal, C.; Kumar Garg, V. (2005). Removal of lead(II) by adsorption using treated granular activated carbon: Batch and column studies. *Journal of Hazardous Materials*, *125*(1–3), 211–220. https://doi.org/10.1016/j.jhazmat.2005.05.032.

[7] Kinuthia, G.K.; Ngure, V.; Beti, D.; Lugalia, R.; Wangila, A., et al. (2020). Levels of heavy metals in wastewater and soil samples from open drainage channels in Nairobi, Kenya: community health implication. *Scientific Reports*, *10*(1), 8434. https://doi.org/10.1038/s41598-020-65359-5.

[8] Yi, Y.M.; Sung, K. (2015). Influence of washing treatment on the qualities of heavy metal–contaminated soil. *Ecological Engineering*, *81*, 89–92.

[9] Ahmed, S.F.; Mofijur, M.; Nuzhat, S.; Chowdhury, A.T.; Rafa, N., et al. (2021). Recent developments in physical, biological, chemical, and hybrid treatment techniques for removing emerging contaminants from wastewater. *Journal of Hazardous Materials*, *416*, 125912. https://doi.org/10.1016/j.jhazmat.2021.125912.

[10] Rizwan, M.S.; Imtiaz, M.; Huang, G.; Chhajro, M.A.; Liu, Y., et al. (2016). Immobilization of Pb and Cu in polluted soil by superphosphate, multi-walled carbon nanotube, rice straw and its derived biochar. *Environmental Science and Pollution Research*, *23*(15), 15532–15543. https://doi.org/10.1007/s11356-016-6695-0.

[11] Yin, K.; Wang, Q.; Lv, M.; Chen, L. (2019). Microorganism remediation strategies towards heavy metals. *Chemical Engineering Journal*, *360*, 1553–1563. https://doi.org/10.1016/j.cej.2018.10.226.

[12] Singh, A.; Pal, D.B.; Mohammad, A.; Alhazmi, A.; Haque, S., et al. (2022). Biological remediation technologies for dyes and heavy metals in wastewater treatment: New insight. *Bioresource Technology*, *343*, 126154. http://doi.org/10.1016/j.biortech.2021.126154.

[13] Shi, L.; Li, J.; Palansooriya, K.N.; Chen, Y.; Hou, D., et al. (2023). Modeling phytoremediation of heavy metal contaminated soils through machine learning. *Journal of Hazardous Materials*, *441*, 129904. https://doi.org/10.1016/j.jhazmat.2022.129904.

[14] Bhayani, D.; Siddhapura, S.P.; Sindhav, S.R.; Jadeja, B.A. (2023). Potentiality of Weed Plants for Phytoremediation of Heavy Metal Polluted Soil. *International Journal of Environment and Climate Change*, *13*(5), 400–412. https://doi.org/10.9734/ijecc/2023/v13i51785.

[15] Njoku, K.L.; Nwani, S.O. (2022). Phytoremediation of heavy metals contaminated soil samples obtained from mechanic workshop and dumpsite using Amaranthus spinosus. *Scientific African*, *17*, e01278. https://doi.org/10.1016/j.sciaf.2022.e01278.

[16] Lin, H.; Liu, C.; Li, B.; Dong, Y. (2021). Trifolium repens L. regulated phytoremediation of heavy metal contaminated soil by promoting soil enzyme activities and beneficial rhizosphere associated microorganisms. *Journal of Hazardous Materials*, *402*, 123829. https://doi.org/10.1016/j.jhazmat.2020.123829.

[17] Bian, F.; Zhong, Z.; Zhang, X.; Yang, C.; Gai, X. (2020). Bamboo – An untapped plant resource for the phytoremediation of heavy metal contaminated soils. *Chemosphere*, *246*, 125750. https://doi.org/10.1016/j.chemosphere.2019.125750.

[18] Ogundiran, M.B.; Ikpeni, S.E. (2018). Metakaolin clay-derived geopolymer for recycling of waste cathode ray tube glass. *African Journal of Pure and Applied Chemistry*, *12*(6), 42–49. https://doi.org/10.5897/AJPAC2018.0759.

[19] Hammer, D.; Kayser, A.; Keller, C. (2003). Phytoextraction of Cd and Zn with Salix viminalis in field trials. *Soil Use and Management*, *19*(3), 187–192. https://doi.org/10.1111/j.1475-2743.2003.tb00303.x.

[20] Gomes, M.A. da C.; Hauser-Davis, R.A.; de Souza, A.N.; Vitória, A.P. (2016). Metal phytoremediation: General strategies, genetically modified plants and applications in metal nanoparticle contamination. *Ecotoxicology and Environmental Safety*, *134*, 133–147. https://doi.org/10.1016/j.ecoenv.2016.08.024.

[21] Mahar, A.; Wang, P.; Ali, A.; Awasthi, M.K.; Lahori, A.H.; et al. (2016). Challenges and opportunities in the phytoremediation of heavy metals contaminated soils: A review. *Ecotoxicology and Environmental Safety*, *126*, 111–121. https://doi.org/10.1016/j.ecoenv.2015.12.023.

[22] LeDuc, D. L.; Terry, N. (2005). Phytoremediation of toxic trace elements in soil and water. *Journal of Industrial Microbiology & Biotechnology*, *32*(11–12), 514–520. https://doi.org/10.1007/s10295-005-0227-0.

[23] Rezaei, A.; Hassani, H.; Hassani, S.; Jabbari, N.; Fard Mousavi, S. B.; et al. (2019). Evaluation of groundwater quality and heavy metal pollution indices in Bazman basin, southeastern Iran. *Groundwater for Sustainable Development*, *9*, 100245. https://doi.org/10.1016/j.gsd.2019.100245.

[24] Vu, T.H.; Gowripalan, N. (2018). Mechanisms of heavy metal immobilisation using geopolymerisation techniques – A review. *Journal of Advanced Concrete Technology*, *16*(3), 124–135. https://doi.org/10.3151/jact.16.124.

[25] Ogundiran, M.B.; Nugteren, H.W.; Witkamp, G.J. (2013). Immobilisation of lead smelting slag within spent aluminate—fly ash based geopolymers. *Journal of Hazardous Materials*, *248–249*, 29–36. https://doi.org/10.1016/j.jhazmat.2012.12.040.

[26] Duxson, P.; Fernández-Jiménez, A.; Provis, J.L.; Lukey, G.C.; Palomo, A.; et al. (2007). Geopolymer technology: the current state of the art. *Journal of Materials Science*, *42*(9), 2917–2933. https://doi.org/10.1007/s10853-006-0637-z.

[27] Guo, B.; Liu, B.; Yang, J.; Zhang, S. (2017). The mechanisms of heavy metal immobilization by cementitious material treatments and thermal treatments: A review. *Journal of Environmental Management*, *193*, 410–422. https://doi.org/10.1016/j.jenvman.2017.02.026.

[28] Zhang, J.; Provis, J.L.; Feng, D.; van Deventer, J.S.J. (2008). Geopolymers for immobilization of Cr^{6+}, Cd^{2+}, and Pb^{2+}. *Journal of Hazardous Materials*, *157*(2–3), 587–598. https://doi.org/10.1016/j.jhazmat.2008.01.053.

[29] Perera, D.S.; Aly, Z.; Vance, E.R.; Mizumo, M. (2005). Immobilization of Pb in a Geopolymer Matrix. *Journal of the American Ceramic Society*, *88*(9), 2586–2588. https://doi.org/10.1111/j.1551-2916.2005.00438.x.

[30] Yunsheng, Z.; Wei, S.; Qianli, C.; Lin, C. (2007). Synthesis and heavy metal immobilization behaviors of slag based geopolymer. *Journal of Hazardous Materials*, *143*(1–2), 206–213. https://doi.org/10.1016/j.jhazmat.2006.09.033.

[31] Qian, G.; Delai Sun, D.; Hwa Tay, J. (2003). Characterization of mercury- and zinc-doped alkali-activated slag matrix. *Cement and Concrete Research*, *33*(8), 1251–1256. https://doi.org/10.1016/S0008-8846(03)00045-0.

[32] Van Jaarsveld, J.G.S.; Van Deventer, J.S.J.; Lorenzen, L. (1997). The potential use of geopolymeric materials to immobilise toxic metals: Part I. Theory and applications. *Minerals Engineering*, *10*(7), 659–669. https://doi.org/10.1016/S0892-6875(97)00046-0.

[33] Šesták, J.; Kočí, V.; Černý, R.; Kovařík, T. (2023). Thirty years since J. Davidovits introduced geopolymers considered now as hypo-crystalline materials within the mers-framework and the

effect of oxygen binding: a review. *Journal of Thermal Analysis and Calorimetry*, *148*(20), 10455–10463. https://doi.org/10.1007/s10973-023-12312-z.

[34] Adeniyi, F.I.; Ogundiran, M.B.; Hemalatha, T.; Hanumantrai, B.B. (2020). Characterization of raw and thermally treated Nigerian kaolinite-containing clays using instrumental techniques. *SN Applied Sciences*, *2*(5), 821. https://doi.org/10.1007/s42452-020-2610-x.

[35] Davidovits, J. (1991). Geopolymers. *Journal of Thermal Analysis*, *37*(8), 1633–1656. https://doi.org/10.1007/BF01912193.

[36] Ogundiran, M. B.; Nugteren, H. W.; Witkamp, G. J. (2016). Geopolymerisation of fly ashes with waste aluminium anodising etching solutions. *Journal of Environmental Management*, *181*, 118–123. https://doi.org/10.1016/j.jenvman.2016.06.017.

[37] El-Eswed, B.I.; Yousef, R.I.; Alshaaer, M.; Hamadneh, I.; Al-Gharabli, S. I.; et al. (2015). Stabilization/solidification of heavy metals in kaolin/zeolite based geopolymers. *International Journal of Mineral Processing*, *137*, 34–42. https://doi.org/10.1016/j.minpro.2015.03.002.

[38] Phair, J.W.; van Deventer, J.S.J.; Smith, J.D. (2004). Effect of Al source and alkali activation on Pb and Cu immobilisation in fly-ash based "geopolymers." *Applied Geochemistry*, *19*(3), 423–434. https://doi.org/10.1016/S0883-2927(03)00151-3.

[39] Nikolić, V.; Komljenović, M.; Marjanović, N.; Baščarević, Z.; Petrović, R. (2014). Lead immobilization by geopolymers based on mechanically activated fly ash. *Ceramics International*, *40*(6), 8479–8488. https://doi.org/10.1016/j.ceramint.2014.01.059.

[40] Palomo, A.; Palacios, M. (2003). Alkali-activated cementitious materials: Alternative matrices for the immobilisation of hazardous wastes. *Cement and Concrete Research*, *33*(2), 289–295. https://doi.org/10.1016/S0008-8846(02)00964-X.

[41] Pandey, B.; Kinrade, S.D.; Catalan, L.J.J (2012). Effects of carbonation on the leachability and compressive strength of cement-solidified and geopolymer-solidified synthetic metal wastes. *Journal of Environmental Management*, *101*, 59–67. https://doi.org/10.1016/j.jenvman.2012.01.029.

[42] Izquierdo, M.; Querol, X.; Davidovits, J.; Antenucci, D.; Nugteren, H.; et al. (2009). Coal fly ash-slag-based geopolymers: Microstructure and metal leaching. *Journal of Hazardous Materials*, *166*(1), 561–566. https://doi.org/10.1016/j.jhazmat.2008.11.063.

[43] Cheng, T.W.; Lee, M.L.; Ko, M.S.; Ueng, T.H.; Yang, S.F. (2012). The heavy metal adsorption characteristics on metakaolin-based geopolymer. *Applied Clay Science*, *56*, 90–96. https://doi.org/10.1016/j.clay.2011.11.027.

[44] Van Jaarsveld, J.G.S.; Van Deventer, J.S.J.; Schwartzman, A. (1999). The potential use of geopolymeric materials to immobilise toxic metals: Part II. Material and leaching characteristics. *Minerals Engineering*, *12*(1), 75–91. https://doi.org/10.1016/S0892-6875(98)00121-6.

[45] El-eswed, B.I. (2020). Chemical evaluation of immobilization of wastes containing Pb, Cd, Cu and Zn in alkali-activated materials: A critical review. *Journal of Environmental Chemical Engineering*, *8*(5), 104194. https://doi.org/10.1016/j.jece.2020.104194.

[46] Li, S.; Huang, X.; Muhammad, F.; Yu, L.; Xia, M.; et al. (2018). Waste solidification/stabilization of lead–zinc slag by utilizing fly ash based geopolymers. *RSC Advances*, *8*(57), 32956–32965. https://doi.org/10.1039/C8RA06634E.

[47] Waijarean, N.; MacKenzie, K.J.D.; Asavapisit, S.; Piyaphanuwat, R.; Jameson, G.N.L. (2017). Synthesis and properties of geopolymers based on water treatment residue and their immobilization of some heavy metals. *Journal of Materials Science*, *52*(12), 7345–7359. https://doi.org/10.1007/s10853-017-0970-4.

[48] El-Eswed, B.I.; Yousef, R.I.; Alshaaer, M.; Hamadneh, I.; Al-Gharabli, S.I.; et al. (2015). Stabilization/solidification of heavy metals in kaolin/zeolite based geopolymers. *International Journal of Mineral Processing*, *137*, 34–42. https://doi.org/10.1016/j.minpro.2015.03.002.

[49] Nikolići, I.; Đurović, D.; Tadić, M.; Blečić, D.; Radmilović, V. (2013). Immobilization of zinc from metallurgical waste and water solutions using geopolymerization technology. *E3S Web of Conferences*, *1*, 41026. https://doi.org/10.1051/e3sconf/20130141026.

[50] Singh, R.; Budarayavalasa, S. (2021). Solidification and stabilization of hazardous wastes using geopolymers as sustainable binders. *Journal of Material Cycles and Waste Management*, *23*(5), 1699–1725. https://doi.org/10.1007/s10163-021-01245-0.

[51] Guo, X.; Shi, H.; Xu, M. (2013). Static and dynamic leaching experiments of heavy metals from fly ash-based geopolymers. *Journal of Wuhan University of Technology-Mater. Sci. Ed.*, *28*(5), 938–943. https://doi.org/10.1007/s11595-013-0797-z.

[52] Palacios, M.; Palomo, A. (2004). Alkali-activated fly ash matrices for lead immobilisation: a comparison of different leaching tests. *Advances in Cement Research*, *16*(4), 137–144. https://doi.org/10.1680/adcr.2004.16.4.137.

[53] Phillip, E.; Choo, T.F.; Khairuddin, N.W.A.; Abdel Rahman, R.O. (2023). On the Sustainable Utilization of Geopolymers for Safe Management of Radioactive Waste: A Review. *Sustainability*, *15*(2), 1117. https://doi.org/10.3390/su15021117.

[54] Petlitckaia, S.; Barré, Y.; Piallat, T.; Grauby, O.; Ferry, D.; et al. (2020). Functionalized geopolymer foams for cesium removal from liquid nuclear waste. *Journal of Cleaner Production*, *269*, 122400. https://doi.org/10.1016/j.jclepro.2020.122400.

[55] Srivastava, S.; Chaudhary, R.; Khale, D. (2008). Influence of pH, curing time and environmental stress on the immobilization of hazardous waste using activated fly ash. *Journal of Hazardous Materials*, *153*(3), 1103–1109. https://doi.org/10.1016/j.jhazmat.2007.09.065.

[56] Ogundiran, M.B., Osibanjo O. (2008). Heavy metal concentrations in soils and accumulation in plants growing in a deserted slag dumpsite in Nigeria. *African Journal of Biotechnology*, *7*, 3053-3060.

[57] Zhang, Z.; Wang, H.; Zhu, Y.; Reid, A.; Provis, J.L.; et al. (2014). Using fly ash to partially substitute metakaolin in geopolymer synthesis. *Applied Clay Science*, *88–89*, 194–201. https://doi.org/10.1016/j.clay.2013.12.025.

[58] Duxson, P.; Provis, J.L. (2008). Designing Precursors for Geopolymer Cements. *Journal of the American Ceramic Society*, *91*(12), 3864–3869. https://doi.org/10.1111/j.1551-2916.2008.02787.x.

[59] Ogundiran, M. B., & Kumar, S. (2015). Synthesis and characterisation of geopolymer from Nigerian Clay. *Applied Clay Science*, *108*, 173–181. https://doi.org/10.1016/j.clay.2015.02.022.

[60] Ogundiran, M.B.; Ikotun, O.J. (2014). Investigating the Suitability of Nigerian Calcined Kaolins as Raw Materials for Geopolymer Binders. *Transactions of the Indian Ceramic Society*, *73*(2), 138–142. https://doi.org/10.1080/0371750X.2014.922430.

[61] Ranjbar, N.; Kuenzel, C.; Spangenberg, J.; Mehrali, M. (2020). Hardening evolution of geopolymers from setting to equilibrium: A review. *Cement and Concrete Composites*, *114*, 103729. https://doi.org/10.1016/j.cemconcomp.2020.103729.

[62] Kaze, C.R.; Djobo, J.N.Y.; Nana, A.; Tchakoute, H.K.; Kamseu, E.; et al. (2018). Effect of silicate modulus on the setting, mechanical strength and microstructure of iron-rich aluminosilicate (laterite) based-geopolymer cured at room temperature. *Ceramics International*, *44*(17), 21442–21450. https://doi.org/10.1016/j.ceramint.2018.08.205.

[63] Their, J.M.; Ozakca, M. (2018). Developing geopolymer concrete by using cold-bonded fly ash aggregate, nano-silica, and steel fiber. *Construction and Building Materials*, *180*, 12–22. https://doi.org/10.1016/j.conbuildmat.2018.05.274.

[64] Malviya, R.; Chaudhary, R. (2006). Factors affecting hazardous waste solidification/stabilization: A review. *Journal of Hazardous Materials*, *137*(1), 267–276. https://doi.org/10.1016/j.jhazmat.2006.01.065.

[65] Chezom, D.; Chimi, K.; Choden, S.; Wangmo, T.; Shashi, D.; et al. (2013). Comparative Study of Different Leaching Procedures. *International Journal of Engineering Research and General Science*, *1*(2).

[66] Ayodele, O.B.; Sulaimon, A.A.; Alaba, P.A.; Tian, Z.Y. (2020). Influence of metakaolinization temperature on the structure and activity of metakaolin supported Ni catalyst in dry methane reforming. *Journal of Environmental Chemical Engineering*, *8*(1), 103239. https://doi.org/10.1016/j.jece.2019.103239.

[67] Barbosa, V.F.; MacKenzie, K.J.; Thaumaturgo, C. (2000). Synthesis and characterisation of materials based on inorganic polymers of alumina and silica: sodium polysialate polymers. *International Journal of Inorganic Materials*, *2*(4), 309–317. https://doi.org/10.1016/S1466-6049(00)00041-6.

[68] Ravisankar, R.; Naseerutheen, A.; Rajalakshmi, A.; Raja Annamalai, G.; Chandrasekaran, A. (2014). Application of thermogravimetry–differential thermal analysis (TG–DTA) technique to study the ancient potteries from Vellore dist, Tamilnadu, India. *Spectrochimica Acta Part A: Molecular and Biomolecular Spectroscopy*, *129*, 201–208. https://doi.org/10.1016/j.saa.2014.02.095

[69] Kim, B.; Lee, S. (2020). Review on characteristics of metakaolin-based geopolymer and fast setting. *Journal of the Korean Ceramic Society*, *57*(4), 368–377. https://doi.org/10.1007/s43207-020-00043-y.

[70] Silva, P. De; Sagoe-Crenstil, K.; Sirivivatnanon, V. (2007). Kinetics of geopolymerization: Role of Al_2O_3 and SiO_2. *Cement and Concrete Research*, *37*(4), 512–518. https://doi.org/10.1016/j.cemconres.2007.01.003.

[71] Siyal, A.A.; Azizli, K.A.; Man, Z.; Ullah, H. (2016). Effects of Parameters on the Setting Time of Fly Ash Based Geopolymers Using Taguchi Method. *Procedia Engineering*, *148*, 302–307. https://doi.org/10.1016/j.proeng.2016.06.624.

[72] Dave, N.; Misra, A.K.; Srivastava, A.; Kaushik, S.K. (2017). Setting time and standard consistency of quaternary binders: The influence of cementitious material addition and mixing. *International Journal of Sustainable Built Environment*, *6*(1), 30–36. https://doi.org/10.1016/j.ijsbe.2016.10.004.

[73] Tian, X.; Xu, W.; Song, S.; Rao, F.; Xia, L. (2020). Effects of curing temperature on the compressive strength and microstructure of copper tailing-based geopolymers. *Chemosphere*, *253*, 126754. https://doi.org/10.1016/j.chemosphere.2020.126754.

[74] Diaz, E.I.; Allouche, E.N.; Eklund, S. (2010). Factors affecting the suitability of fly ash as source material for geopolymers. *Fuel*, *89*(5), 992–996. https://doi.org/10.1016/j.fuel.2009.09.012.

[75] Xu H.; Lukey G.C.; van Deventer, J.S.J. (2004). The Activation of Class C-, Class F-Fly Ash and Blast Furnace Slag Using Geopolymerisation. the proceedings of the Eighth CANMET/ACI International Conference on Fly Ash, Silica Fume, Slag, and Natural Pozzolan, SP-221.

[76] Wijaya, L.A.; Jaya Ekaputri, J.; Triwulan (2017). Factors influencing strength and setting time of fly ash based-geopolymer paste. *MATEC Web of Conferences*, *138*, 01010. https://doi.org/10.1051/matecconf/201713801010.

[77] Seo, J.; Park, S.; Yoon, H.N.; Lee, H.K. (2020). Effect of CaO incorporation on the microstructure and autogenous shrinkage of ternary blend Portland cement-slag-silica fume. *Construction and Building Materials*, *249*, 118691. https://doi.org/10.1016/j.conbuildmat.2020.118691.

[78] Elimbi, A.; Tchakoute, H.K.; Njopwouo, D. (2011). Effects of calcination temperature of kaolinite clays on the properties of geopolymer cements. *Construction and Building Materials*, *25*(6), 2805–2812. http://doi.org/10.1016/j.conbuildmat.2010.12.055.

[79] Standard Specification for building Brick (Solid Masonry Units Made from Clay or Shale). (accessed on 2 January 2024) Available online: https://www.astm.org/c0062-17.html.

[80] Abbass, W.; Abbas, S.; Aslam, F.; Ahmed, A.; Ahmed, T.; et al. (2022). Manufacturing of Sustainable Untreated Coal Ash Masonry Units for Structural Applications. *Materials*, *15*(11), 4003. https://doi.org/10.3390/ma15114003.

[81] Oladele, O.L.; Adesanya, E.D.; Arbe, A.; Iturrospe, A.; Ogundiran, M.B. (2023). Mitigation of efflorescence, drying shrinkage and water demand of calcined clay-based geopolymers with biological waste ashes as activator and hardener. *Applied Clay Science*, *243*, 107050. https://doi.org/10.1016/j.clay.2023.107050.

[82] Chen, X.; Zhang, J.; Lu, M.; Chen, B.; Gao, S.; et al. (2022). Study on the effect of calcium and sulfur content on the properties of fly ash based geopolymer. *Construction and Building Materials*, *314*, 125650. https://doi.org/10.1016/j.conbuildmat.2021.125650.

[83] Mahmoodi, O.; Siad, H.; Lachemi, M.; Dadsetan, S.; Sahmaran, M. (2021). Development and characterization of binary recycled ceramic tile and brick wastes-based geopolymers at ambient and high temperatures. *Construction and Building Materials*, *301*, 124138. https://doi.org/10.1016/j.conbuildmat.2021.124138.

[84] Duxson, P.; Lukey, G.C.; Separovic, F.; van Deventer, J.S.J. (2005). Effect of Alkali Cations on Aluminum Incorporation in Geopolymeric Gels. *Industrial & Engineering Chemistry Research*, *44*(4), 832–839. https://doi.org/10.1021/ie0494216.